Brain tissue iron neurophysiology and its relationship with the cognitive effects of dopaminergic modulation in children with and without ADHD

Arianna D. Cascone [a,*], Finnegan Calabro [b,c], William Foran [b], Bart Larsen [d], Tehila Nugiel [e], Ashley C. Parr [b], Brenden Tervo-Clemmens [f], Beatriz Luna [b], Jessica R. Cohen [e,g,h]

[a] Neuroscience Curriculum, School of Medicine, University of North Carolina at Chapel Hill, Chapel Hill, NC, USA
[b] Department of Psychiatry, University of Pittsburgh, Pittsburgh, PA, USA
[c] Department of Bioengineering, University of Pittsburgh, Pittsburgh, PA, USA
[d] Department of Psychiatry, Perelman School of Medicine, University of Pennsylvania, Philadelphia, PA, USA
[e] Carolina Institute for Developmental Disabilities, University of North Carolina at Chapel Hill, Chapel Hill, NC, USA
[f] Department of Psychiatry, Massachusetts General Hospital, Harvard Medical School, Boston, MA, USA
[g] Department of Psychology and Neuroscience, University of North Carolina at Chapel Hill, Chapel Hill, NC, USA
[h] Biomedical Research Imaging Center, University of North Carolina at Chapel Hill, Chapel Hill, NC, USA

ARTICLE INFO

ABSTRACT

Children with attention-deficit/hyperactivity disorder (ADHD) exhibit impairments in response inhibition. These impairments are ameliorated by modulating dopamine (DA) via the administration of rewards or stimulant medication like methylphenidate (MPH). It is currently unclear whether intrinsic DA availability impacts these effects of dopaminergic modulation on response inhibition. Thus, we estimated intrinsic DA availability using magnetic resonance-based assessments of basal ganglia and thalamic tissue iron in 36 medication-naïve children with ADHD and 29 typically developing (TD) children (8–12 y) who underwent fMRI scans and completed standard and rewarded go/no-go tasks. Children with ADHD additionally participated in a double-blind, randomized, placebo-controlled, crossover MPH challenge. Using linear regressions covarying for age and sex, we determined there were no group differences in brain tissue iron. We additionally found that higher putamen tissue iron was associated with worse response inhibition performance in all participants. Crucially, we observed that higher putamen and caudate tissue iron was associated with greater responsivity to MPH, as measured by improved task performance, in participants with ADHD. These results begin to clarify the role of subcortical brain tissue iron, a measure associated with intrinsic DA availability, in the cognitive effects of reward- and MPH-related dopaminergic modulation in children with ADHD and TD children.

1. Introduction

Attention-deficit/hyperactivity disorder (ADHD) is one of the most common neurodevelopmental disorders of childhood, affecting 5–10% of children worldwide (Danielson et al., 2018; Polanczyk et al., 2007). ADHD is characterized by developmentally inappropriate levels of inattention, hyperactivity, and impulsivity (American Psychiatric Association, 2013). These core symptoms are often accompanied by deficits in cognitive control, a set of goal-directed processes involved in regulating thoughts and behaviors (Diamond, 2013). One domain of cognitive control that is typically impaired in ADHD is response inhibition (Castellanos et al., 2006; Diamond, 2013; Luman et al., 2005); individuals with ADHD exhibit difficulty suppressing actions that may

interfere with goal-directed behaviors (Lijffijt et al., 2005; Mostofsky and Simmonds, 2008; Oosterlaan et al., 1998). These response inhibition deficits put individuals with ADHD at risk for negative long-term outcomes, including substance use disorders and criminal behavior (Diamond, 2013; DuPaul et al., 2001; DuPaul and Stoner, 2014; Fletcher and Wolfe, 2009; Philipp-Wiegmann et al., 2018).

Studies of the neural etiology of response inhibition deficits in ADHD have focused on the neurotransmitter dopamine, given its established role in modulating frontostriatal circuits important for response inhibition (Fusar-Poli et al., 2012; Haber and Knutson, 2010; Nieoullon, 2002; Volkow et al., 2009). It is thought that dopamine's actions in distinct cortical-basal ganglia loops redirect information from ventromedial frontostriatal networks involved in reward processing to

---

dorsolateral frontostriatal networks involved in cognitive control (Arnsten and Rubia, 2012; Haber, 2003; Spanagel and Weiss, 1999). Previous neuroimaging research suggests that dopamine neurotransmission is dysfunctional in individuals with ADHD (Fusar-Poli et al., 2012). Positron emission tomography (PET) studies have shown that dopamine metabolism, receptor availability, and transporter function is disrupted in adults and children with ADHD (Ernst et al., 1999; Volkow et al., 2009, 2011). Magnetic resonance imaging (MRI) studies have further shown that children and adults with ADHD exhibit reduced activation and functional connectivity in frontostriatal regions and networks during tasks that probe attention and response inhibition (Cubillo et al., 2010; Rubia et al., 2009).

Previous research has demonstrated that modulation of the dopaminergic system improves the symptoms and cognitive deficits related to ADHD, including response inhibition (Epstein et al., 2011; Ma et al., 2016; Rosch et al., 2016; Tamm and Carlson, 2007). In fact, the receipt of rewards during laboratory tasks has been shown to improve response inhibition performance in individuals with ADHD and in age- and sex-matched typically developing (TD) controls (Ma et al., 2016). This reward-related reinforcement increases synaptic availability of dopamine in the striatum (Arnsten and Rubia, 2012). Further, the psychostimulant methylphenidate (MPH), the current first-line treatment for ADHD, is an indirect dopamine and norepinephrine agonist. Due to MPH's dopamine agonism via blockage of dopamine transporters, extracellular levels of striatal dopamine increase following MPH administration (Faraone, 2018; Volkow, Fowler, et al., 2002a, 2002b; Volkow, Wang et al., 2002). Examining how response inhibition performance changes following the receipt of rewards and MPH administration, and how these performance changes relate to indirect measures of dopamine availability, will therefore shed light on the neurobiological mechanisms through which dopaminergic modulation improves response inhibition in both individuals with ADHD and TD children.

Research assessing dopaminergic functioning and dopamine availability in humans in vivo is limited, especially in children, because techniques such as PET involve the use of radiation (Brix et al., 2005). One way to circumvent this limitation and indirectly assess dopamine availability in the brain is with magnetic resonance-based measurements of brain tissue iron. Iron is a cofactor of the rate-limiting enzyme tyrosine hydroxylase and of monoamine oxidase, both of which are critical for dopamine synthesis (Nagatsu et al., 1964). In the human brain, iron is preferentially sequestered in regions that make up the brain's dopaminergic reward pathway, including the basal ganglia and thalamus (Brass et al., 2006; Hallgren and Sourander, 1958; Ortega et al., 2007). These regions are also critical components of the aforementioned frontostriatal circuitry involved in response inhibition and reward-related reinforcement (Haber and Knutson, 2010). Since the presence of iron increases the rate of T2* relaxation, quantifying the T2* relaxation rate (i.e., R2*) of functional MRI (fMRI) data can be used to measure basal ganglia tissue iron levels (Haacke et al., 2005, 2010). Indeed, previous work has employed this approach to investigate basal ganglia iron content by estimating the relative T2* relaxation rate across the brain using existing fMRI data (Larsen and Luna, 2015; Peterson et al., 2019; Price et al., 2021). Recent neuroimaging work using PET has confirmed that midbrain tissue iron measurements derived by quantifying the T2* relaxation rate are correlated with dopamine availability in the striatum, specifically with presynaptic vesicular storage of dopamine (Kilbourn, 2014; Larsen, Olafsson et al., 2020).

Few studies to date have leveraged brain tissue iron measurements to probe dopaminergic function in individuals with ADHD. These studies have found that individuals with ADHD exhibit reduced brain tissue iron levels in the basal ganglia and thalamus relative to their age- and sex-matched TD peers (Adisetiyo et al., 2014; Cortese et al., 2012; Hasaneen et al., 2017), which is in line with other neuroimaging work finding reduced midbrain dopamine activity in ADHD (Volkow et al., 2009). None of these studies have examined the relationship between dopamine-related brain tissue iron neurophysiology and response

inhibition performance in individuals with ADHD. Even so, research suggests that greater levels of brain tissue iron are associated with better cognitive ability in TD children (Hect et al., 2018), adolescents, and young adults (Larsen, Bourque et al., 2020), as well as with responsivity to the receipt of rewards during a response inhibition task in TD adolescents and adults (Parr et al., 2022). However, the question of whether these relationships are consistent in individuals with ADHD, and whether dopamine-related physiology modulates the response to dopaminergic modulation in ADHD, remains.

The overarching goal of this pre-registered project, therefore, is to investigate brain tissue iron content in the basal ganglia and thalamus using time-averaged normalized T2*-weighted (nT2*w) signal and to assess whether variability in the nT2*w measurement is related to responsivity to dopaminergic modulation in children with ADHD and TD children. Here, 'dopaminergic modulation' refers to reward reinforcement or administration of MPH, and responsivity to this modulation will be operationalized as improvement on tasks probing response inhibition. As prior work has found that individuals with ADHD have lower basal ganglia and thalamic tissue iron levels relative to their TD peers (Adisetiyo et al., 2014; Cortese et al., 2012; Hasaneen et al., 2017), we predict that individuals with ADHD will have higher nT2*w signal, reflecting reduced brain tissue iron levels, in these regions. Based on previous work in TD individuals (Hect et al., 2018; Larsen, Bourque et al., 2020; Parr et al., 2022), we hypothesize that individuals with lower nT2*w signal, reflecting greater tissue iron levels, will exhibit better response inhibition, as well as greater improvements in response inhibition following the administration of rewards and MPH.

2. Materials and methods

2.1. Participants

The dataset for the proposed study is a subset of 65 participants with ADHD and TD participants between the ages of 8–12 years who participated in a larger study assessing the effects of MPH administration on functional brain network organization (ADHD: n = 36, 17 F, mean age = 9.70 y; TD: n = 29, 12 F, mean age = 10.23 y). Participants were selected for inclusion in the current study based on fMRI and behavioral data quality. See *Motion-related quality assurance* and *Go/no-go tasks and measures* for details about data quality criteria for fMRI and behavioral data, respectively. General exclusion criteria for the sample included full scale intelligence quotient (FSIQ) less than 85 as determined using the Wechsler Intelligence Scale for Children, Fifth Edition (WISC-V; Wechsler, 2014), Word Reading subtest score less than 85 from the Wechsler Individual Achievement Test, Third Edition (WIAT-III; Wechsler, 1992), or if any of the following conditions were met: (a) diagnosis of intellectual disability, developmental speech/language disorder, reading disability, autism spectrum disorder, or a pervasive developmental disorder; (b) visual or hearing impairment; (c) neurologic disorder (e.g., epilepsy, cerebral palsy, traumatic brain injury, Tourette syndrome); (d) medical contraindication to MRI (e.g., implanted electrical devices, dental braces). Diagnostic status was assessed using the Diagnostic Interview Schedule for Children Version IV (DISC-IV; Shaffer et al., 2000) and the Conners 3rd Edition Parent and Teacher Rating Scales (Conners-3; Conners et al., 2011). Participants were included in the ADHD group if they met: (a) full diagnostic criteria for ADHD on the DISC-IV, or (b) intermediate diagnostic criteria (i.e., subthreshold with impairment) on the DISC-IV and full diagnostic criteria for ADHD on the Conners-3 Parent or Teacher Rating Scales. They were additionally required to be psychostimulant medication naïve. Participants were included in the TD group if they met the above criteria and did not meet diagnostic criteria for any psychiatric disorders, including ADHD, on the DISC-IV. Additionally, TD participants were required to have three or fewer symptoms of inattention and of hyperactivity/impulsivity on the DISC-IV. Finally, TD participants were required to have no history or presence of developmental disorders, and

no history or presence of ADHD in first-degree relatives. A demographic summary including age, FSIQ as determined using the WISC-V, Word Reading subtest score from the WIAT-III, sex, race, family income, and parental education, is provided in Table 1.

2.2. Procedures

All procedures for the parent study were reviewed and approved by the Institutional Review Board at the University of North Carolina at Chapel Hill. Written parental consent and participant (child) assent were obtained for each participant included in the larger study. Only procedures relevant to the proposed analyses will be described here. Participants underwent two fMRI sessions approximately one week apart (mean = 10.4 days; standard deviation = 7.4 days; range = 3–42 days). Since attention fluctuates throughout the day in school-aged children (Escribano and Díaz-Morales, 2014), most sessions were scheduled at approximately the same time of day (i.e., between 8 am – 12 pm). Seven TD sessions (12.5%) and 16 ADHD sessions (23%) were scheduled in the afternoon. There was not a significant difference across groups in terms of when sessions were scheduled ($c^2(1) = 2.4$, $p = .13$). Two participants with ADHD and two TD participants only participated in a single session. Each MRI session included an MPRAGE anatomical T1-weighted scan and the following T2*-weighted echo-planar imaging (EPI) functional scans: two resting-state scans (five minutes each), two standard go/no-go task scans (6.5 min each), and four rewarded go/no-go task scans (six minutes each), administered in that order. During the resting-state scans, participants viewed a white fixation cross on a gray background and were instructed to lie quietly, but awake, in the MRI scanner. For the go/no-go task scans, stimuli were projected onto a screen visible to the participant through a mirror mounted to the head coil and an MRI-safe handheld button box was used to record task responses. Both tasks were presented using PsychoPy v1.85.1 (Peirce, 2007, 2009). Both fMRI sessions were identical for participants in the TD group. In the case that a TD child had usable fMRI and behavioral data from both sessions, data from the session with the highest percentage of fMRI volumes retained after motion scrubbing were used, based on fMRI data exclusion criteria (See *Motion-related quality assurance*).

Participants in the ADHD group participated in a double-blind, randomized, placebo-controlled crossover MPH challenge. On each day of testing, participants in the ADHD group received 0.30 mg/kg MPH or placebo, rounded up to the nearest 5 mg, orally approximately one hour before scanning. Aside from the MPH challenge, fMRI sessions for participants in the ADHD group were identical. Since we were interested in how intrinsic, baseline brain tissue iron levels are related to improvements in response inhibition that follow dopaminergic modulation, such as the receipt of rewards during cognitive tasks or the administration of MPH, fMRI data collected following placebo administration were used to assess brain tissue iron in all analyses for children with ADHD. Furthermore, it has been proposed that brain tissue iron estimates derived from fMRI are reflective of stable properties of brain tissue (Larsen and Luna, 2015; Price et al., 2021), and we confirmed that this was the case in our data, both across sessions in TD children (i.e., across a weeks-long period) and between placebo and MPH sessions in children with ADHD (i.e., after a single dose of MPH; see Supplementary Materials, *Supplementary analyses* and *Supplementary results,* Fig. S1, Table S1). In the analyses that examined responsivity to rewards only, behavioral data collected following placebo administration were used. In the analyses that examined the effects of MPH administration, behavioral data collected following both placebo and MPH administration were used. All analyses here were pre-registered and the protocol was submitted to Open Science Framework prior to data analysis.

2.3. Go/no-go tasks and measures

Two versions of a go/no-go task, a standard and a rewarded version, were administered. The versions of the go/no-go task we used were adapted from one that was initially designed to have a high proportion of errors (Winter and Sheridan, 2014). In both versions, eight sports balls were used as the stimuli. Two of the eight sports balls were randomly selected for each participant as 'no-go' stimuli. The other six sports balls were 'go' stimuli. Participants were instructed to respond as quickly as possible with a button press using their right index finger following the presentation of 'go' sports balls (73.4% of trials) and to withhold responding when 'no-go' sports balls were presented (26.6% of trials).

Table 1
Demographic Characteristics.

	ADHD (n = 36)	TD (n = 29)	Corrected *p*-values
Age in years, mean (SD)	9.70 (1.18)	10.23 (1.51)	0.44
FSIQ[a], mean (SD)	113.2 (12.6)	116.8 (11.8)	0.53
Word Reading[b], mean (SD)	113.6 (10.6)	116.0 (10.5)	0.44
Sex (M/F)	19/17	17/12	0.74
Race			0.87
Asian	2	2	
Black/African American	1	1	
White/Caucasian	30	25	
Multiracial	3	1	
Family Income			0.44
< $24,999	1	1	
$25,000-$74,999	6	3	
> $75,000	28	22	
Don't know/did not respond	1	3	
Parental Education			0.44
High school diploma/GED	4	1	
Associate degree	1	0	
Bachelor's degree	15	7	
Master's degree	7	9	
Doctoral or professional degree	8	12	
Did not respond	1	0	

Frequencies are presented for race, family income, and parental education categories. Two typically developing (TD) participants did not complete the WISC-IV or WIAT-III (M, 8.2 y; M, 10.4 y). Welch's t-tests for unequal variance were used to compare groups on age, FSIQ, and word reading scores. Two-sample chi-squared tests were used to compare groups on sex, race, family income, and parental education. Tests were FDR-corrected for seven comparisons.

[a] FSIQ derived from the Wechsler Intelligence for Children, Fifth Edition (WISC-V, Wechsler, 2014).

[b] Word reading (standard score) derived from the Wechsler Individual Achievement Test, 3rd addition (WIAT-III, Wechsler, 1992).
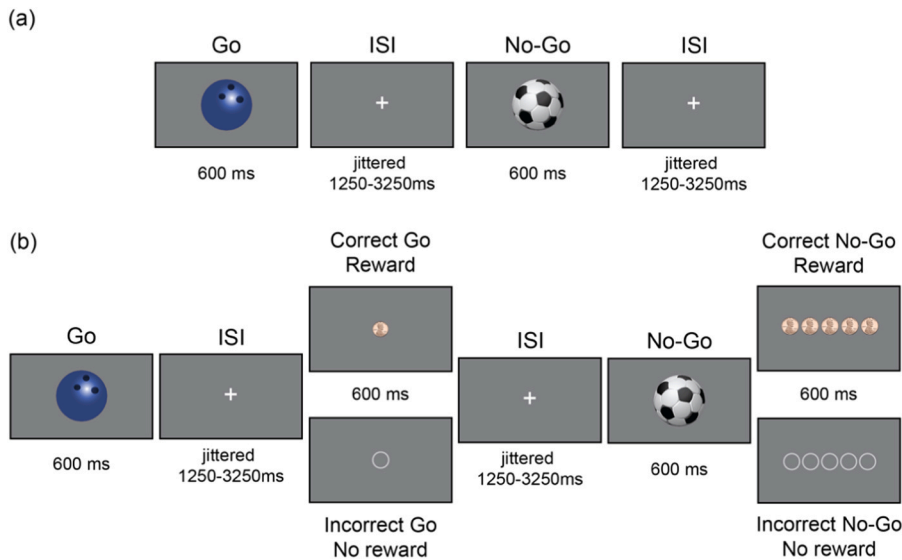
Fig. 1. Standard and rewarded go/no-go tasks. (a) Standard go/no-go task. Sports-ball stimuli were shown individually for 600 ms each. In this example, the bowling ball is the 'go' stimulus and the soccer ball is the 'no-go' stimulus. (b) Rewarded go/no-go task. Sports-ball stimuli were followed by a feedback screen in which the reward that was earned (top, pennies) or not earned (bottom, empty circles) was shown. One penny was earned for each correct go trial, and five pennies were earned for each correct no-go trial. ISI = interstimulus interval; ms = milliseconds.

The standard go/no-go task (Fig. 1a) consisted of two runs of 128 trials each, for a total of 256 trials (188 go trials and 68 no-go trials). Stimulus order was pseudorandom such that between two and four go trials preceded each no-go trial. There were 16 instances of two consecutive go trials, 10 instances of three consecutive go trials, and eight instances of four consecutive go trials, randomized for each run. Each stimulus was presented for 600 ms, with a jittered interstimulus interval (ISI) of 1250–3250 ms selected from a uniform distribution. In the rewarded go/no-go task (Fig. 1b), stimuli and timing were identical to the standard go/no-go task, with the addition of feedback after each response. Feedback (coins for correct trials and empty circles for incorrect trials) was presented for 600 ms after a brief delay that was jittered identically to the ISI between trials. Due to the longer trial length, the rewarded go/no-go task consisted of four runs of 64 trials each, again for a total of 256 trials. The instructions for the rewarded go/no-go task were identical to the standard version, but participants were also told that they would be rewarded for correct, fast responses on go trials (≤ 650 ms) and for correct non-responses on no-go trials. Participants received one penny per correct/fast go trial and five pennies per correct no-go trial. Participants received the money they accumulated over the four runs of the rewarded go/no-go task at the end of each visit.

Individual runs of the standard and rewarded go/no-go tasks were excluded for an omission rate on go trials that was greater than three standard deviations from the mean omission error rate, separately for each task, as determined using standard and rewarded go/no-go task data collected from participants with ADHD following placebo administration and TD participants. Specifically, individual runs of the standard go/no-go task were excluded if the proportion of omission errors exceeded 0.44 and individual runs of the rewarded go/no-go task were excluded if the proportion of omission errors exceeded 0.39. This was to ensure that participants were awake and actively engaging with the task. Additionally, individual go trials with response times faster than 200 ms were excluded from analyses, as exceptionally fast response times are indicative of anticipatory responses (Cragg and Nation, 2008). Behavioral performance was indexed using the proportion of commission errors and response time variability. The proportion of commission errors was calculated as the proportion of no-go trials on which a response was made. Response time variability was quantified using tau, which is derived from the exponential-Gaussian distributional model of response times and assesses infrequent, extremely slow response times that are indicative of attention lapses (Leth-Steensen et al., 2000). Tau quantifies the mean and standard deviation of the exponential component of the response time distribution. To calculate tau, the timefit function from

the 'retimes' package in R (Massidda, 2013) was used to bootstrap the response times associated with correct go trials 5000 times, and the mean and standard deviation of the exponential distribution of response times was calculated. For summary statistics of behavioral performance, see Table S2 in Supplementary Materials.

The distributions of the proportion of commission errors and tau were assessed for normality using the Shapiro-Wilk test of normality ($\alpha = 0.05$) (Shapiro and Wilk, 1965). Tau was not normally distributed, and the proportion of commission errors on the standard go/no-go task in all participants and following MPH administration in participants with ADHD was not normally distributed (all p-values < 0.04; see Supplementary Materials, Table S3). Therefore, log-transformed values of both the proportion of commission errors and tau were used in all analyses.

2.4. MRI data acquisition

All neuroimaging data were collected at the University of North Carolina at Chapel Hill Biomedical Research Imaging Center. Data were acquired with a 32-channel head coil on a 3-Tesla Siemens MAGNETOM Prisma-fit whole-body MRI machine. High resolution T1-weighted anatomical scans were acquired using a magnetization prepared rapid acquisition gradient echo (MPRAGE) sequence (TR = 2400 ms, TE = 2.22 ms, FA = 8°, field of view 256 × 256 mm, 208 slices, resolution = 0.8 mm × 0.8 mm × 0.8 mm). Whole-brain T2*-weighted fMRI data were acquired using an echo-planar imaging (EPI) sequence (39 axial slices parallel to the AC–PC line, slice thickness 3 mm, interslice distance = 3.3 mm, TR = 2000 ms, TE = 25 ms, FA = 77°, echo spacing = 0.54 ms, field of view 230 mm × 230 mm, voxel dimensions: 2.9 mm × 2.9 mm × 3.0 mm). For the resting-state scan, 300 timepoints were collected (150 timepoints and five minutes per each of two runs). A total of 390 timepoints were collected during the standard go/no-go task (195 timepoints and 6.5 min per each of two runs), and 740 timepoints were collected during the rewarded go/no-go task (185 timepoints and 6.17 min per each of four runs).

2.5. fMRIPrep anatomical and functional data preprocessing

The following text has been adapted from the fMRIPrep boilerplate text that is automatically generated with the express intention that it is used in manuscripts. It is released under the CC0 license.

All T1w images were corrected for intensity non-uniformity (INU) with N4BiasFieldCorrection (Tustison et al., 2010) and distributed with

ANTs 2.2.0 (Avants et al., 2008, RRID:SCR_004757). The T1w reference was then skull-stripped with a Nipype implementation of the ants-BrainExtraction.sh workflow (from ANTs), using OASIS30ANTs as the target template. Brain tissue segmentation of cerebrospinal fluid (CSF), white matter (WM), and gray matter (GM) was performed on the brain-extracted T1w using FAST (FSL 5.0.9, RRID:SCR_002823, Zhang et al., 2001). A T1w-reference map was computed after registration and INU-correction of the T1w images used mri_robust_template (FreeSurfer 6.0.1, Reuter et al., 2010). Brain surfaces were reconstructed using recon-all (FreeSurfer 6.0.1, RRID:SCR_001847, Dale et al., 1999), and the brain mask estimated previously was refined with a custom variation of the method to reconcile ANTs- and FreeSurfer-derived segmentations of the cortical gray matter of Mindboggle (RRID:SCR_002438, Klein et al., 2017). Volume-based spatial normalization to standard MNI152NLin2009cAsym space was performed via nonlinear registration with antsRegistration (ANTs 2.2.0), using brain-extracted versions of both the T1w reference and the T1w template. ICBM 152 Nonlinear Asymmetrical template version 2009c was selected for spatial normalization (Fonov et al., 2009, RRID:SCR_008796; TemplateFlow ID: MNI152NLin2009cAsym).

For each subject's BOLD runs (across all tasks and sessions), the following preprocessing was performed. First, a reference volume and its skull-stripped version was generated using a custom methodology of fMRIPrep. A deformation field to correct for susceptibility distortions was estimated based on fMRIPrep's fieldmap-less approach. The deformation field resulted from coregistering the BOLD reference to the same-subject T1w reference with its intensity inverted (Huntenburg, Freie, 2014; Wang et al., 2017). Registration was performed with antsRegistration (ANTs 2.2.0), and the process was regularized by constraining deformation to be nonzero only along the phase-encoding direction and modulated with an average fieldmap template (Treiber et al., 2016). Based on the estimated susceptibility distortion, an unwarped BOLD reference was calculated for a more accurate coregistration with the anatomical reference. The BOLD reference was then coregistered to the T1w reference using bbregister (FreeSurfer), which implements boundary-based registration (Greve and Fischl, 2009). Coregistration was configured with six degrees of freedom. Head-motion parameters with respect to the BOLD reference (transformation matrices, and six corresponding rotation and translation parameters) were estimated using MCFLIRT (FSL 5.0.9, Jenkinson et al., 2012). BOLD runs were slice-time corrected using 3dTshift from AFNI 20160207 (Cox and Hyde, 1997, RRID:SCR_005927). The BOLD timeseries (including slice-timing correction) were resampled onto their original, native space by applying a single, composite transform to correct for head-motion and susceptibility distortions. These resampled BOLD timeseries will be referred to as preprocessed BOLD in original space, or just preprocessed BOLD. The preprocessed BOLD timeseries were then resampled into standard space, generating a preprocessed BOLD run in MNI152N-Lin2009cAsym space. A reference volume and its skull-stripped version were generated using a custom methodology of fMRIPrep.

Following the processing and resampling steps, confounding framewise displacement (FD) timeseries were calculated based on the preprocessed BOLD for each functional run, using implementations in Nipype (following the definition by Power et al., 2014). Many internal operations of fMRIPrep use Nilearn 0.5.2 (Abraham et al., 2014, RRID: SCR_001362), mostly within the functional processing workflow. For more details of the pipeline, see the section corresponding to workflows in fMRIPrep's documentation.

2.6. Normalization and time-averaging of T2*-weighted data

In this set of analyses, BOLD signal was not used since we did not perform a timeseries analyses. Instead, we were interested in iron levels, which are a time-invariant property of brain tissue quantified from T2*-weighted data (Larsen and Luna, 2015; Peterson et al., 2019; Price et al., 2021; Vo et al., 2011).

To quantify normalized T2*-weighted (nT2*w) signal, first high motion timepoints were removed and subsequently excluded from analyses. High motion timepoints were defined as those that exceeded 0.3 mm FD (Parr et al., 2022; Siegel et al., 2014). Then, to correct for scanner drift and potential differences between participants and MRI runs, each volume was normalized to the whole brain mean. The nT2*w signal from each voxel was then aggregated across all remaining volumes of the resting-state and task runs using the median, separately for each participant. The median was used to reduce the impact of outlier volumes (Parr et al., 2022). This resulted in a voxel-wise map of median nT2*w signal for each participant. As the presence of iron is inversely related to nT2*w signal, reduced nT2*w signal indicates increased brain tissue iron and therefore increased intrinsic DA availability.

2.7. ROI selection

Bilateral caudate, putamen, globus pallidus, accumbens, and thalamus were selected as regions of interest. These regions were selected for two reasons. First, they are dopamine rich, and iron is colocalized with dopamine in the brain (Beard, 2003; Haber and Knutson, 2010; Schipper, 2012). Second, reduced brain tissue iron has been observed in each of these regions in children with ADHD relative to age- and sex-matched TD peers (Adisetiyo et al., 2014; Cortese et al., 2012; Hasaneen et al., 2017).

ROIs were defined using the Harvard-Oxford subcortical atlas (Jenkinson et al., 2012). ROIs only included voxels with at least 50% probability of belonging to each specific brain region. NT2*w signal was averaged across all voxels in each ROI, resulting in a single value per ROI. We first analyzed nT2*w signal across a whole basal ganglia ROI and a thalamus ROI. The basal ganglia ROI combined Harvard-Oxford atlas masks of bilateral caudate, putamen, globus pallidus, and accumbens into a single basal ganglia ROI. Next, to assess the regional specificity of basal ganglia nT2*w signal and its relationships with performance, we extracted nT2*w signal from bilateral caudate, putamen, globus pallidus, and accumbens separately.

2.8. Motion-related quality assurance

Any participant with at least 170 volumes remaining across all fMRI runs after excluding high motion timepoints was included in the current study (Larsen and Luna, 2015). One participant with ADHD was excluded as their fMRI data following placebo administration did not meet this criterion. To ensure that nT2*w signal was not significantly impacted by motion, we correlated mean FD across all runs with the nT2*w signal for each region of interest (ROI) using Pearson correlations ($\alpha = 0.05$). There were no significant relationships between mean FD and nT2*w signal in any of the ROIs we examined (all corrected p-values > 0.48; see Supplementary Materials, Table S4).

2.9. Analyses

Before conducting each of the below analyses, power analyses were performed to determine statistical power to detect the expected effects. See Supplementary Materials, *Expected Power* for details.

Group comparisons of demographic variables: To ensure that the ADHD and TD groups did not differ on demographic variables, including sex, race, family income, and parental education, we used two-sample chi-squared tests to compare groups on each of these variables. We additionally conducted Welch's t-tests for unequal variance to compare groups on age, FSIQ, and Word Reading scores. Tests were FDR-corrected for seven comparisons at p < .05.

Replication analysis – comparing nT2*w signal in children with ADHD and TD children: We first replicated previous work and examined whether there were group differences between children with ADHD and TD children in nT2*w signal in the whole basal ganglia and thalamus (Adisetiyo et al., 2014; Cortese et al., 2012; Hasaneen et al., 2017). We

used separate linear regression models covaring for age and sex for each of the two ROIs, as follows:

nT2*w signal ~ group + age + sex

Models were FDR-corrected for two comparisons at p < . 05 (Benjamini and Hochberg, 1995). We also determined whether there were group differences in nT2*w signal in specific basal ganglia subregions (i. e., caudate, putamen, globus pallidus, and accumbens). In this secondary analysis, we again used separate linear regression models covaring for age and sex for each of the four ROIs. Here, results were FDR-corrected for four comparisons at p < .05 (Benjamini and Hochberg, 1995). One participant with ADHD was not included in this analysis as their fMRI data following placebo administration had fewer than 170 volumes included after excluding high-motion timepoints (See *Motion-related quality assurance*). This left 64 participants ($n_{ADHD} = 35$, $n_{TD} = 29$) in this analysis.

Relationship between nT2*w signal and response inhibition: To determine the relationship between nT2*w signal and response inhibition in children with ADHD and TD children, we used linear regression models covaring for age and sex using the following equation:

response inhibition performance ~ nT2*w signal + age + sex

For the primary analysis, we used separate linear regression models for each response inhibition performance measure (commission errors, tau) and ROI (whole basal ganglia and thalamus) for a total of four models (two response inhibition measures x two ROIs). Statistical tests were FDR-corrected for two comparisons separately for each response inhibition measure at p < .05, as we included two ROIs in the primary analysis (Benjamini and Hochberg, 1995).

In a secondary analysis that assessed regional specificity of the relationship between nT2*w signal and response inhibition performance, we extracted nT2*w signal from each basal ganglia ROI separately. We used separate linear regression models for each response inhibition performance measure (commission errors, tau) and basal ganglia ROI (caudate, putamen, globus pallidus, and accumbens) for a total of eight models (two response inhibition measures x four ROIs). Here, statistical tests were FDR-corrected for four comparisons separately for each response inhibition measure at p < .05, as we included four basal ganglia ROIs (Benjamini and Hochberg, 1995).

Given literature indicating that the relationship between brain tissue iron and response inhibition performance is strongest in individuals with high levels of brain tissue iron (Parr et al., 2022), and that individuals with ADHD have reduced brain tissue iron relative to TD individuals (Adisetiyo et al., 2014; Cortese et al., 2012; Hasaneen et al., 2017), we performed an additional analysis in which we examined whether the relationship between nT2*w signal and response inhibition performance differed as a function of diagnostic group. As such, we implemented linear regression models wherein response inhibition performance was predicted by nT2*w signal, diagnostic group, and the interaction between nT2*w signal and diagnostic group, covaring for age and sex as follows:

response inhibition performance ~ nT2*w signal + group + nT2*w signal*-group + age + sex

Separate linear regression models for each response inhibition measure and ROI were used, and groups of models were FDR-corrected separately at p < .05 as above (i.e., two corrections per response inhibition measure for whole basal ganglia and thalamus in the primary analysis; four corrections per response inhibition measure for caudate, putamen, globus pallidus, and accumbens in the secondary analysis).

One additional participant was not considered for inclusion in this analysis due to inconsistent presentation of no-go stimuli (n = 1, TD). This left 63 participants ($n_{ADHD} = 35$, $n_{TD} = 28$) in this analysis.

Relationship between nT2*w signal and responsivity to reward: To examine whether variability in nT2*w signal predicts responsivity to reward in children with ADHD and TD children, change in performance from the standard go/no-go task to the rewarded go/no-go task was calculated for all participants by subtracting performance measures on the rewarded go/no-go task from those on the standard go/no-go task, such that higher values (i.e., more positive) reflected greater improvements in task performance. Linear regression models covaring for age and sex were used to relate nT2*w signal to change in response inhibition performance separately for each response inhibition measure and ROI using the following equation:

Δ response inhibition performance ~ nT2*w signal + age + sex

As in the analyses above, separate linear regression models for each response inhibition measure and ROI were used. Again, groups of models were FDR-corrected separately at p < .05 (Benjamini and Hochberg, 1995). Specifically, for the primary analysis, two corrections per response inhibition measure (commission errors, tau) were made for the whole basal ganglia and thalamus. In the secondary analysis, four corrections per response inhibition measure were made for the basal ganglia subregions (i.e., caudate, putamen, globus pallidus, and accumbens).

We also performed an additional analysis that examined whether the relationship between nT2*w signal and responsivity to reward differed as a function of diagnostic group. As such, we implemented linear regression models wherein change in response inhibition performance was predicted by nT2*w signal, diagnostic group, and the interaction between nT2*w signal and diagnostic group, covaring for age and sex as follows:

Δresponse inhibition performance ~ nT2*w signal + group + nT2*w signal*group + age + sex

Separate linear regression models covaring for age and sex for each response inhibition measure and ROI were used. Models were FDR-corrected in the same way as described in the previous analyses at p < .05 (Benjamini and Hochberg, 1995). That is, for each response inhibition measure (commission errors, tau) two corrections were made in the primary analysis that examined nT2*w signal in the basal ganglia and thalamus, and four corrections were made in the secondary analysis that examined nT2*w signal in the four basal ganglia subregions (i.e., caudate, putamen, globus pallidus, and accumbens).

Two additional participants were not considered for inclusion in this analysis for missing rewarded go/no-go data (n = 1, TD) and incorrect button presses during the rewarded go/no-go task (n = 1, ADHD), leaving 61 participants ($n_{ADHD} = 34$, $n_{TD} = 27$) in this analysis.

Relationship between nT2*w signal and responsivity to MPH: To investigate whether variability in nT2*w signal predicts responsivity to MPH in children with ADHD, change in standard go/no-go performance from placebo to MPH was calculated by subtracting performance measures on MPH from those on placebo. Here, higher values (i.e., more positive) indicate greater improvement of performance following MPH. Linear regression models covaring for age and sex were used to relate nT2*w signal to change in response inhibition performance separately for each response inhibition measure and ROI using the following equation:

Δ response inhibition performance ~ nT2*w signal + age + sex

As in the previous analyses, statistical tests were FDR-corrected separately for each response inhibition measure at p < .05 (Benjamini and Hochberg, 1995). In the primary analysis, statistical tests were corrected for two comparisons per response inhibition measure (commission errors, tau), as there were two ROIs (whole basal ganglia and thalamus). In the secondary analysis, statistical tests were corrected for four comparisons per response inhibition measure, as there were four basal ganglia subregion ROIs (caudate, putamen, globus pallidus, and accumbens).

Three participants with ADHD were not considered for inclusion in

this analysis for missing standard go/no-go data on placebo (n = 1) and on MPH (n = 2), leaving 33 participants in this analysis.

For all linear regression models, standardized betas are reported in the *Results* section.

3. Results

3.1. Group comparisons of demographic variables

There were no significant differences between the ADHD and TD groups on age, FSIQ, word reading scores, sex, race, family income, or parental education (all corrected p-values > 0.44; Table 1).

3.2. Replication analysis – comparing nT2*w signal in children with ADHD and TD children

There were no significant group differences in nT2*w signal in the whole basal ganglia and thalamus ROIs or in the individual basal ganglia ROIs (i.e., caudate, putamen, globus pallidus, and accumbens) (all corrected p-values > 0.52; see Supplementary Materials Fig. S2, Table S5).

3.3. Relationship between nT2*w signal and response inhibition

First, we examined the relationship between nT2*w signal and response inhibition performance on the standard go/no-go task in all participants. There were no significant relationships between nT2*w signal in the whole basal ganglia or thalamus ROIs and the proportion of commission errors (both corrected p-values > 0.15; Fig. 2a-b). When assessing the regional specificity of the relationship between nT2*w signal and the proportion of commission errors, lower nT2*w signal (i.e., higher brain tissue iron) in the putamen was significantly related to higher proportion of commission errors ($\beta = -0.13$, corrected p-value = .04; Fig. 2c). There were no significant relationships between nT2*w signal of the caudate, globus pallidus, or accumbens and the proportion of commission errors (all corrected p-values > 0.24; Fig. 2d, Supplementary Materials, Figs. S7, S8). When relating nT2*w signal to tau, no relationships were significant (all corrected p-values > 0.83). For parameter estimates and plots of relationships with tau and of additional ROIs, see Supplementary Materials, Table S6, Figs. S3, S7, S8.

In additional analyses that examined group differences in the relationship between nT2*w signal in the whole basal ganglia and thalamus ROIs and the proportion of commission errors and tau, we did not observe significant interaction effects (both corrected p-values for proportion of commission errors > 0.67; both corrected p-values for tau > 0.17). We similarly did not observe significant interaction effects when examining each basal ganglia ROI separately (all corrected p-values for proportion of commission errors > 0.62; all corrected p-values for tau > 0.10). For parameter estimates, see Supplementary Materials, Table S7.

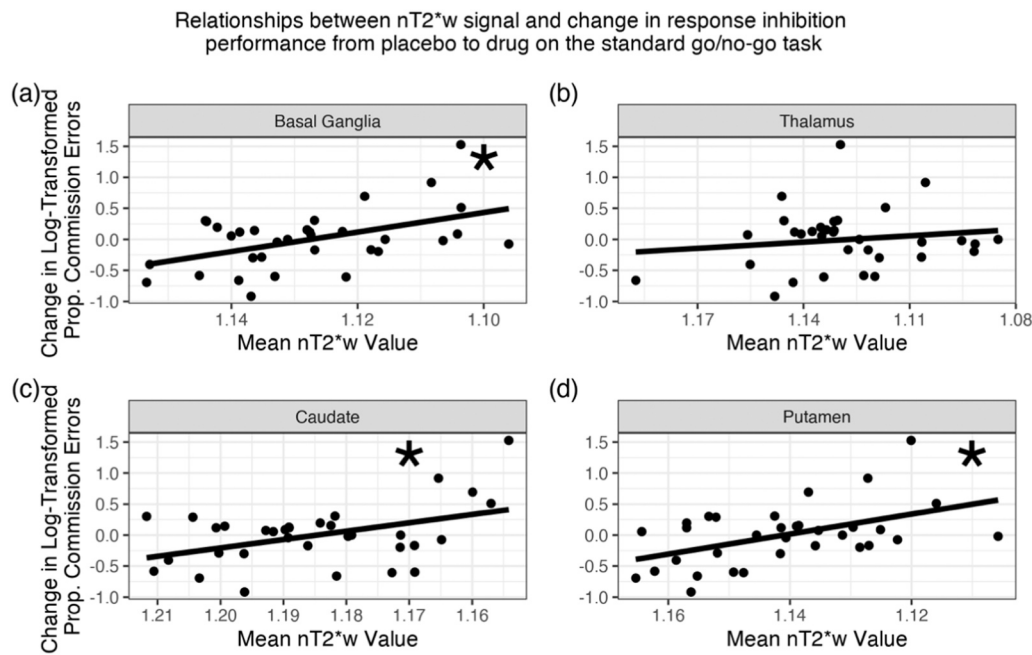### 3.4. Relationship between nT2*w signal and responsivity to reward

Next, we examined whether there was a relationship between nT2*w signal and responsivity to reward in all participants. We operationalized responsivity to reward as the change in performance (i.e., the proportion of commission errors or tau) between the standard and rewarded go/no-go task (standard go/no-go – rewarded go/no-go). There were no significant relationships between nT2*w signal in the basal ganglia or thalamus and responsivity to reward as measured by change in proportion of commission errors (both corrected p-values > 0.20; Fig. S4a-b). Further, there were no significant relationships between nT2*w signal in any of the subregions of the basal ganglia (i.e., caudate, putamen, globus pallidus, and accumbens) and change in proportion of commission errors (all corrected p-values > 0.25; Fig. S4c-d, Supplementary Materials, Figs. S7, S8). When relating nT2*w signal to change in tau, no relationships were significant (all corrected p-values > 0.43). For parameter estimates and plots of relationships with tau and of additional ROIs, see Supplementary Materials, Table S8, Figs. S4, S5, S7, S8.

In additional analyses that examined group differences in the relationship between nT2*w signal in the whole basal ganglia and thalamus ROIs and the change in proportion of commission errors and tau, we did not observe significant interaction effects (both corrected p-values for proportion of commission errors > 0.07; both corrected p-values for tau > 0.96). We similarly did not observe significant interaction effects when examining each basal ganglia ROI separately (all corrected p-values for proportion of commission errors > 0.06; all corrected p-values for tau > 0.38). For parameter estimates, see Supplementary Materials, Table S9.
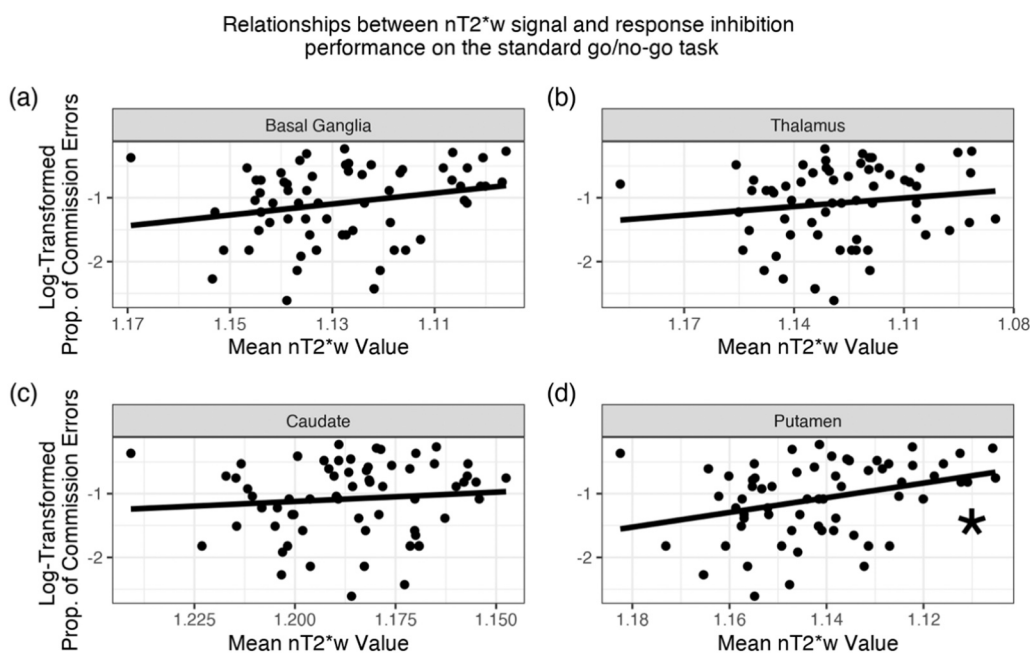
Fig. 2. Relationship between nT2*w signal in the basal ganglia, thalamus, caudate, and putamen and response inhibition performance on the standard go/no-go task. In all panels, for ease of interpretation, the x-axes are reversed to reflect the inverse relationship between nT2*w values and tissue iron, such that values closer to the right of the graph indicate higher brain tissue iron. Lower nT2*w signal (i.e., higher brain tissue iron) in the putamen was significantly related to higher proportion of commission errors (panel (d), corrected p-value = .04). Asterisks indicate FDR-corrected p-value < .05. See Supplementary Materials, Table S6 for all model parameters.

Relationships between nT2*w signal and change in response inhibition performance from placebo to drug on the standard go/no-go task

Fig. 3. Relationship between nT2*w signal in the basal ganglia, thalamus, caudate, and putamen and responsivity to MPH. Responsivity to MPH here is indexed via change in the proportion of commission errors from placebo to MPH (placebo – drug). Positive change therefore indicates that performance improved following drug administration. In all panels, for ease of interpretation, the x-axes are reversed to reflect the inverse relationship between nT2*w values and tissue iron, such that values closer to the right of the graph indicate higher brain tissue iron. Lower basal ganglia nT2*w signal (i.e., higher brain tissue iron) was significantly related to greater improvements in the proportion of commission errors following MPH administration (panel (a), corrected p-value = .01; Table S10). Lower nT2*w signal (i.e., higher brain tissue iron) in the caudate and putamen was significantly related to greater improvements in the proportion of commission errors following MPH administration (caudate: panel (c), corrected p-value = .005, putamen: panel (d), corrected p-value = .01). Asterisks indicate FDR-corrected p-value < .05. See Supplementary Materials, Table S10 for all model parameters.

3.5. Relationship between nT2*w signal and responsivity to MPH

We then examined whether there was a relationship between nT2*w signal and responsivity to MPH in children with ADHD. Responsivity to MPH was defined as a change in the proportion of commission errors or tau on the standard go/no-go task from placebo to MPH (placebo – drug). There was a significant relationship between nT2*w signal in the basal ganglia and change in the proportion of commission errors ($\beta = -0.47$, corrected p-value = .01; Fig. 3a). That is, lower basal ganglia nT2*w signal (i.e., higher brain tissue iron) was significantly related to greater improvements in the proportion of commission errors on MPH. There was not a significant relationship between nT2*w signal in the thalamus and change in proportion of commission errors (corrected p-value > 0.26; Fig. 3b). In secondary analyses examining each basal ganglia subregion separately, there were significant relationships between nT2*w signal in the caudate and in the putamen and change in proportion of commission errors (caudate: $\beta = -0.56$, corrected p-value = .005; putamen: $\beta = -0.47$, corrected p-value = .01; Fig. 3c-d). There were no significant relationships between nT2*w signal in the globus pallidus or accumbens and change in proportion of commission errors (both corrected p-values > 0.26; Supplementary Materials, Figs. S7, S8). When relating nT2*w signal to change in tau, no relationships were significant (all corrected p-values > 0.06). For parameter estimates and plots of relationships with tau and of additional ROIs, see Supplementary Materials, Table S10, Figs. S6-8.

4. Discussion

The main goal of this study was to examine how brain tissue iron levels in the basal ganglia and thalamus related to the cognitive effects of dopaminergic modulation in children with ADHD and TD children. While we did not find significant group differences in basal ganglia or thalamic brain tissue iron, we did observe that tissue iron levels in the putamen related to proportion of commission errors on the standard go/no-go task. Critically, tissue iron levels in the whole basal ganglia, and specifically in the putamen and caudate, were significantly related to

improvements in proportion of commission errors on the standard go/no-go task following MPH administration in children with ADHD.

First, in both registered and unregistered supplementary validation analyses, we confirmed that brain tissue iron measurements are stable over a weeks-long period in TD children and following a one-time MPH challenge in children with ADHD (see Supplementary Materials). Prior work has demonstrated that brain tissue iron measurements are stable over a months-long period in children (Parr et al., 2022) and minutes- and days-long periods in adults (Price et al., 2021). We are the first to show that brain tissue iron measurements in children are indeed stable when assessed approximately one week apart. Additionally, previous work has shown that brain tissue iron levels normalize as a function of chronic psychostimulant treatment (Adisetiyo et al., 2019). We have now confirmed that there is no change in brain tissue iron following a single administration of MPH. As such, our work represents a crucial contribution to the literature.

We did not find significant differences in brain tissue iron in the basal ganglia or thalamus between children with ADHD and TD children. Existing literature is inconsistent in this regard, likely due to the methods used to quantify brain tissue iron. For example, Adisetiyo and colleagues (2014) leveraged both MRI relaxation rates, as implemented here, and magnetic field correlation (MFC). They only observed group differences using MFC-derived measures of brain tissue iron. Further, the ages of our study participants (i.e., 8–12 y) cover a narrower range than other studies, whose ages cover at a minimum 8–14 years (Adisetiyo et al., 2014; Cortese et al., 2012; Hasaneen et al., 2017). Adolescence is a period of significant change within cortical and subcortical dopamine systems (Padmanabhan and Luna, 2014; Wahlstrom et al., 2010), and these changes can be observed using T2*-weighted imaging (Larsen and Luna, 2015; Larsen, Bourque et al., 2020; Larsen, Olafsson et al., 2020). It is therefore possible that differences in brain tissue iron levels between children with ADHD and TD children may not emerge until adolescence.

In addition to examining whether there were group differences in brain tissue iron, we examined relationships between brain tissue iron and response inhibition performance. Previous research examining the

relationships between brain tissue iron and cognition have shown that greater levels of brain tissue iron were related to faster processing speed and higher general intelligence (Hect et al., 2018), as well as greater verbal reasoning, nonverbal reasoning, and spatial processing (Larsen et al., 2020). Though previous work has not focused specifically on response inhibition, we hypothesized that we would similarly find that greater levels of brain tissue iron would be related to better cognitive performance in our study. Instead, we found that higher brain tissue iron in the putamen was related to more commission errors (i.e., worse response inhibition performance) on the standard go/no-go task. Though this significant relationship was specific to the putamen, the general direction of these relationships was largely consistent across brain regions examined. This finding is consistent with literature that has examined the interplay between the dopamine system and response inhibition using other indices of dopamine functioning (Mink, 1996). For example, reduced D2/D3 receptor availability in the caudate and putamen and increased spontaneous eye-blink rate, both of which indicate increased extracellular dopamine levels, have been related to poorer response inhibition performance on the stop-signal task (i.e., increased stop-signal reaction times) (Colzato et al., 2009; Ghahremani et al., 2012). The present study is therefore in line with previous work, as our results suggest that increased dopamine levels as indexed by increased putamen tissue iron are related to more commission errors (i. e., poorer performance) on the standard go/no-go task. Our findings and others' are also in line with models of striatal behavioral control that characterize 'go' (direct) and 'no-go' (indirect) pathways of the basal ganglia (Frank et al., 2007). Specifically, increased dopamine levels are hypothesized to bias the balance toward the 'go' pathway and suppress the 'no-go' pathway (Frank, 2005; Frank et al., 2007), which would result in increased commission errors, as we observed in our study.

In children with ADHD, we found that higher basal ganglia tissue iron levels were associated with greater responsivity to MPH, as indexed by a greater reduction in commission errors on the standard go/no-go task. When focusing on specific basal ganglia subregions, this result was driven by significant relationships in the caudate and putamen. The caudate and putamen are key regions in the cortical-basal ganglia loops associated with cognitive control broadly (Arnsten and Rubia, 2012; Tekin and Cummings, 2002) and response inhibition specifically (Zandbelt and Vink, 2010). Dopaminergic activity in these regions has also been related to the ADHD phenotype (i.e., inattentive symptoms) (Volkow et al., 2007) and to performance improvements following reward in healthy individuals (Calabro et al., 2023). The observations that participants with higher brain tissue iron levels exhibited more commission errors, as well as that children with ADHD with higher brain tissue iron levels exhibited the greatest reduction in commission errors following MPH, suggest that medication effects on response inhibition might be related to response inhibition performance at baseline (i.e., on placebo). Recent work in children with ADHD shows that inhibitory control improvements following MPH administration were greatest in those with the poorest baseline inhibitory control (Fosco et al., 2021). We confirmed this was the case in our data via an unregistered exploratory analysis in which we conducted a linear regression model predicting change in commission errors (placebo – drug) from baseline commission errors (placebo), controlling for age and sex. We found that children with ADHD with the most commission errors on the standard go/no-go task on placebo improved the most following MPH (β =.95, p = .01). Notably, these findings are consistent with prior literature observing that individuals with higher intrinsic DA are more responsive to MPH (Castellanos et al., 1996; Volkow, Fowler et al., 2002b), including reduction of symptoms and improvement of cognitive functioning (Castellanos et al., 1996; Hofmans et al., 2020). Even so, it has been shown that the relationships between intrinsic DA and cognition improvements following MPH administration depend on the specific domains of cognitions examined (Clatworthy et al., 2009; Frank and Fossella, 2011). As such, additional investigations of the precise dopaminergic mechanisms through which MPH improves response inhibition

across individuals with varying levels of intrinsic, baseline DA are needed.

The administration of MPH and the receipt of rewards are both known to improve cognition (Rosch et al., 2016) via their impact on the dopamine system (Arnsten and Rubia, 2012). While recent work has shown that individuals with high levels of brain tissue iron display greater responsivity to dopaminergic modulation via the receipt of rewards (Parr et al., 2022), we did not observe this in our data. Crucially, however, we did observe that the relationships between brain tissue iron and the reduction in commission errors from the standard to rewarded go/no-go task were in the same direction as those observed in analyses that examined responsivity to MPH. Thus, this is generally consistent with prior work suggesting that the receipt of rewards and MPH modulate dopamine similarly by increasing its synaptic availability in the striatum (Arnsten and Rubia, 2012; Faraone, 2018; Volkow, Fowler et al., 2002a, 2002b; Volkow, Wang et al., 2002). Notably, prior literature has reported greater striatal activation in the presence of both MPH and rewards relative to the presence of reward alone (Furukawa et al., 2020) and that MPH administration results in greater improvements in cognitive performance relative to reward-related reinforcement (Rosch et al., 2016), corresponding to a greater effect size (d = 1.54 for MPH (Rosch et al., 2016) and d = 0.60 for rewards (Shiels-- Rosch, Hawk, 2013). Thus, a larger sample may have been needed to detect the smaller effect of rewards on response inhibition. This highlights the need to replicate these results in a larger sample of children with and without ADHD.

We did not observe significant relationships between brain tissue iron and response time variability as indexed by tau on the standard go/ no-go task, nor between brain tissue iron and responsivity to reward or MPH. Response time variability is thought to index a range of cognitive processes, including attention (Leth-Steensen et al., 2000) and working memory (Rapport et al., 2008). Larsen and colleagues (2020) did not find relationships between brain tissue iron and the 'executive control' cognitive domain of the Penn computerized neurocognitive battery, which is defined as abstraction and mental flexibility, attention, and working memory (Gur et al., 2010, 2012). Our results are therefore consistent with this work and suggest that the relationships between brain tissue iron and response inhibition performance might be specific to the ability to withhold responding (i.e., stopping), which is better captured via commission error quantification.

Though our findings contribute to the growing body of evidence that brain tissue iron neurophysiology is linked to cognition in children with ADHD and TD children, there are certain limitations that must be acknowledged. First, it is important to recognize that iron is not a direct measure of all aspects of dopamine function but is most associated with presynaptic dopamine availability (Larsen et al., 2020). Larsen and colleagues (2020) showed that brain tissue iron measurements derived from tissue relaxation rates were significantly associated with PET-derived presynaptic vesicular dopamine storage although not in a 1:1 manner. Iron is important in several biological processes that are not limited to the dopaminergic system, including myelination and production of other catecholamines (Nagatsu et al., 1964). While the basal ganglia is unique in its predominance of DA, it is not a direct measure and results should be interpreted with this limitation in mind. Regardless, leveraging tissue relaxation to quantify dopamine indirectly in children with ADHD and TD children is a promising avenue of research, given the radiation exposure associated with PET imaging (Brix et al., 2005) and subsequent challenges of assessing dopamine levels in vivo in children. Additionally, we did not collect daily serum iron data from participants in the present study. Given the dynamic nature of peripheral iron levels (Hare et al., 2013), the relationship between serum iron and brain tissue iron is difficult to quantify. Even so, it has been shown that serum iron levels do not differ between individuals with and without ADHD (Donfrancesco et al., 2013), so it is unlikely that our results are driven by differences in serum iron level. However, future studies should investigate whether serum iron level relates to cognitive

performance and responsivity to dopaminergic manipulation as we have here with brain tissue iron. We also did not collect sleep data from our participants. We therefore cannot determine whether variability in response inhibition performance in this sample is due to variability in sleep duration or quality. To combat the possibility of sleep differences impacting our results to the best of our ability, we excluded individual runs of the standard and rewarded go/no-go tasks based on omission error rates to ensure that subjects were awake and responding to the task, as described in *Go/no-go tasks and measures*. Finally, MPH is an indirect dopamine and norepinephrine agonist (Faraone, 2018). We were therefore not able to determine whether modulation of the norepinephrine system impacted improvements in response inhibition following the administration of MPH. Additional investigations into the precise neural mechanisms through which MPH improves cognition are needed to answer this question.

In conclusion, while we did not observe significant differences in basal ganglia or thalamic tissue iron in children with ADHD and TD children aged 8–12 y, we did validate the assumption that tissue iron is stable across a weeks-long period in TD children and following a one-time MPH challenge in children with ADHD. We additionally demonstrated that increased tissue iron in the putamen was significantly related to increased commission errors on the standard go/no-go task, and that increased tissue iron in the caudate and putamen, as well as generally in the whole basal ganglia, was significantly related to improvements in the proportion of commission errors following MPH administration. These relationships were not observed when response inhibition performance was indexed using tau (i.e., response time variability). Together, these findings augment existing literature that examines brain tissue iron and its relationships with cognition in children with ADHD and TD children and is one of the first to clarify the role of brain tissue iron in the cognitive effects of dopaminergic modulation. This work is a crucial step toward understanding the mechanisms of both behavioral and medication treatment for ADHD. Further, the present findings suggest that noninvasive brain tissue iron measurements may represent a biomarker for response to dopaminergic treatment in ADHD.

Declaration of Competing Interest

The authors declare that they have no known competing financial interests or personal relationships that could have appeared to influence the work reported in this paper.

Data Availability

This study's protocol was registered via Open Science Framework (https://osf.io/37qr9/). Data was collected as part of an ongoing National Institutes of Health (NIH) grant and will be made available after completion of the study per NIH data sharing requirements (R00MH102349).

Acknowledgments

Appendix A. Supporting information

Supplementary data associated with this article can be found in the online version at doi:10.1016/j.dcn.2023.101274.

References

Abraham, A., Pedregosa, F., Eickenberg, M., Gervais, P., Mueller, A., Kossaifi, J., Gramfort, A., Thirion, B., Varoquaux, G., 2014. Machine learning for neuroimaging with scikit-learn. Front. Neuroinform. Vol. 8 https://doi.org/10.3389/fninf.2014.00014.

Adisetiyo, V., Gray, K.M., Jensen, J.H., Helpern, J.A., 2019. Brain iron levels in attention-deficit/hyperactivity disorder normalize as a function of psychostimulant treatment duration. NeuroImage. Clinical 24, 101993. https://doi.org/10.1016/j.nicl.2019.101993.

Adisetiyo, V., Jensen, J.H., Tabesh, A., Deardorff, R.L., Fieremans, E., Di Martino, A., Gray, K.M., Castellanos, F.X., Helpern, J.A., 2014. Multimodal MR imaging of brain iron in attention deficit hyperactivity disorder: a noninvasive biomarker that responds to psychostimulant treatment? Radiology 272 (2), 524–532. https://doi.org/10.1148/radiol.14140047.

American Psychiatric Association. 2013. Diagnostic and statistical manual of mental disorders (5th ed.).

Arnsten, A.F.T., Rubia, K., 2012. Neurobiological circuits regulating attention, cognitive control, motivation, and emotion: disruptions in neurodevelopmental psychiatric disorders. J. Am. Acad. Child Adolesc. Psychiatry 51 (4), 356–367. https://doi.org/10.1016/j.jaac.2012.01.008.

Avants, B.B., Epstein, C.L., Grossman, M., Gee, J.C., 2008. Symmetric diffeomorphic image registration with cross-correlation: Evaluating automated labeling of elderly and neurodegenerative brain. Med. Image Anal. 12 (1), 26–41. https://doi.org/10.1016/j.media.2007.06.004.

Beard, J., 2003. Iron deficiency alters brain development and functioning. J. Nutr. 133 (5 Suppl 1), 1468S–1472SS. https://doi.org/10.1093/jn/133.5.1468S.

Benjamini, Y., Hochberg, Y., 1995. Controlling the false discovery rate: A practice and powerful approach to multiple testing. Journal of the Royal Statistical Society. Series B (Methodological) 57 (1), 289–300. http://www.jstor.org/stable/2346101.

Brass, S.D., Chen, N., Mulkern, R.V., Bakshi, R., 2006. Magnetic resonance imaging of iron deposition in neurological disorders. Top. Magn. Reson. Imaging 17 (1). ⟨https://journals.lww.com/topicsinmri/Fulltext/2006/02000/Magnetic_Resonance_Imaging_of_Iron_Deposition_in.4.aspx⟩.

Brix, G., Lechel, U., Glatting, G., Ziegler, S.I., Münzing, W., Müller, S.P., Beyer, T., 2005. Radiation exposure of patients undergoing whole-body dual-modality 18F-FDG PET/CT examinations. J. Nucl. Med.: Off. Publ., Soc. Nucl. Med. 46 (4), 608–613.

Calabro, F.J., Montez, D.F., Larsen, B., Laymon, C.M., Foran, W., Hallquist, M.N., Price, J.C., Luna, B., 2023. Striatal dopamine supports reward expectation and learning: A simultaneous PET/fMRI study. NeuroImage 267, 119831. https://doi.org/10.1016/j.neuroimage.2022.119831.

Castellanos, F.X., Elia, J., Kruesi, M.J.P., Marsh, W.L., Gulotta, C.S., Potter, W.Z., Ritchie, G.F., Hamburger, S.D., Rapoport, J.L., 1996. Cerebrospinal fluid homovanillic acid predicts behavioral response to stimulants in 45 boys with attention deficit/hyperactivity disorder. Neuropsychopharmacology 14 (2), 125–137. https://doi.org/10.1016/0893-133X(95)00077-Q.

Castellanos, F.X., Sonuga-Barke, E.J.S., Milham, M.P., Tannock, R., 2006. Characterizing cognition in ADHD: beyond executive dysfunction. Trends Cogn. Sci. 10 (3), 117–123. https://doi.org/10.1016/j.tics.2006.01.011.

Clatworthy, P.L., Lewis, S.J.G., Brichard, L., Hong, Y.T., Izquierdo, D., Clark, L., Cools, R., Aigbirhio, F.I., Baron, J.-C., Fryer, T.D., Robbins, T.W., 2009. Dopamine release in dissociable striatal subregions predicts the different effects of oral methylphenidate on reversal learning and spatial working memory. J. Neurosci.: Off. J. Soc. Neurosci. 29 (15), 4690–4696. https://doi.org/10.1523/JNEUROSCI.3266-08.2009.

Colzato, L.S., Van Den Wildenberg, Van Wouwe, Pannebakker, M.M., Hommel, B., 2009. Dopamine and inhibitory action control: Evidence from spontaneous eye blink rates. Experimental Brain Research 196 (3), 467–474. https://doi.org/10.1007/s00221-009-1862-x.

Conners, C.K., Pitkanen, J., Rzepa, S.R., 2011. Conners. In: Kreutzer, J.S., DeLuca, J., Caplan, B. (Eds.), Encyclopedia of Clinical Neuropsychology, 3rd edition.,. Springer, New York, pp. 675–678. https://doi.org/10.1007/978-0-387-79948-3_1534.

Cortese, S., Azoulay, R., Castellanos, F.X., Chalard, F., Lecendreux, M., Chechin, D., Delorme, R., Sebag, G., Sbarbati, A., Mouren, M.-C., Bernardina, B.D., Konofal, E., 2012. Brain iron levels in attention-deficit/hyperactivity disorder: a pilot MRI study. World J. Biol. Psychiatry 13 (3), 223–231. https://doi.org/10.3109/15622975.2011.570376.

Cox, R.W., Hyde, J.S., 1997. Software tools for analysis and visualization of fMRI data. NMR Biomed. 10 (4–5), 171–178. https://doi.org/10.1002/(sici)1099-1492(199706/08)10:4/5<171::aid-nbm453>3.0.co;2-l.

Cragg, L., Nation, K., 2008. Go or no-go? developmental improvements in the efficiency of response inhibition in mid-childhood. Dev. Sci. 11 (6), 819–827. https://doi.org/10.1111/j.1467-7687.2008.00730.x.

Cubillo, A., Halari, R., Ecker, C., Giampietro, V., Taylor, E., Rubia, K., 2010. Reduced activation and inter-regional functional connectivity of fronto-striatal networks in adults with childhood Attention-Deficit Hyperactivity Disorder (ADHD) and persisting symptoms during tasks of motor inhibition and cognitive switching. Journal of psychiatric research 44 (10), 629–639. https://doi.org/10.1016/j.jpsychires.2009.11.016.

Dale, A.M., Fischl, B., Sereno, M.I., 1999. Cortical surface-based analysis: I. Segmentation and surface reconstruction. NeuroImage 9 (2), 179–194. https://doi.org/10.1006/nimg.1998.0395.

Danielson, M.L., Bitsko, R.H., Ghandour, R.M., Holbrook, J.R., Kogan, M.D., Blumberg, S.J., 2018. Prevalence of parent-reported ADHD diagnosis and related treatment about US children and adolescents. J. Clin. Child Adolesc. Psychol. 47 (2), 199–212.

Diamond, A., 2013. Executive functions. Annu. Rev. Psychol. 64 (1), 135–168. https://doi.org/10.1146/annurev-psych-113011-143750.

Donfrancesco, R., Parisi, P., Vanacore, N., Martines, F., Sargentini, V., Cortese, S., 2013. Iron and ADHD: time to move beyond serum ferritin levels. J. Atten. Disord. 17 (4), 347–357. https://doi.org/10.1177/1087054711430712.

DuPaul, G.J., Stoner, G., 2014. ADHD in the Schools: Assessment and Intervention Strategies. Guilford Publications,.

DuPaul, G.J., McGoey, K.E., Eckert, T.L., VanBrakle, J., 2001. Preschool children with attention-deficit/hyperactivity disorder: impairments in behavioral, social, and school functioning. J. Am. Acad. Child Adolesc. Psychiatry 40 (5), 508–515. https://doi.org/10.1097/00004583-200105000-00009.

Epstein, J.N., Langberg, J.M., Rosen, P.J., Graham, A., Narad, M.E., Antonini, T.N., Brinkman, W.B., Froehlich, T., Simon, J.O., Altaye, M., 2011. Evidence for higher reaction time variability for children with ADHD on a range of cognitive tasks including reward and event rate manipulations. Neuropsychology 25 (4), 427.

Ernst, M., Zametkin, A.J., Jons, P.H., Matochik, J.A., Pascualvaca, D., Cohen, R.M., 1999. High presynaptic dopaminergic activity in children with Tourette's disorder. J. Am. Acad. Child Adolesc. Psychiatry 38 (1), 86–94.

Escribano, C., Díaz-Morales, J.F., 2014. Daily fluctuations in attention at school considering starting time and chronotype: An exploratory study. Chronobiol. Int. 31 (6), 761–769. https://doi.org/10.3109/07420528.2014.898649.

Faraone, S.V., 2018. The pharmacology of amphetamine and methylphenidate: relevance to the neurobiology of attention-deficit/hyperactivity disorder and other psychiatric comorbidities. Neurosci. Biobehav. Rev. 87, 255–270. https://doi.org/10.1016/j.neubiorev.2018.02.001.

Fletcher, J., Wolfe, B., 2009. Long-term consequences of childhood ADHD on criminal activities. J. Ment. Health Policy Econ. 12 (3), 119–138.

Fonov, V.S., Evans, A.C., McKinstry, R.C., Almli, C.R., Collins, D.L., 2009. Unbiased nonlinear average age-appropriate brain templates from birth to adulthood. NeuroImage 47, S102. https://doi.org/10.1016/S1053-8119(09)70884-5.

Fosco, W.D., Rosch, K.S., Waxmonsky, J.G., Pelham, W.E., Hawk, L.W., 2021. Baseline performance moderates stimulant effects on cognition in youth with ADHD. Experimental and Clinical Psychopharmacology 29 (4), 302–307. https://doi.org/10.1037/pha0000374.

Frank, M.J., 2005. Dynamic dopamine modulation in the basal ganglia: a neurocomputational account of cognitive deficits in medicated and nonmedicated Parkinsonism. J. Cogn. Neurosci. 17 (1), 51–72. https://doi.org/10.1162/0898929052880093.

Frank, M.J., Fossella, J.A., 2011. Neurogenetics and pharmacology of learning, motivation, and cognition. Neuropsychopharmacology 36 (1), 133–152. https://doi.org/10.1038/npp.2010.96.

Frank, M.J., Santamaria, A., O'Reilly, R.C., Willcutt, E., 2007. Testing computational models of dopamine and noradrenaline dysfunction in attention deficit/hyperactivity disorder. Neuropsychopharmacol.: Off. Publ. Am. Coll. Neuropsychopharmacol. 32 (7), 1583–1599. https://doi.org/10.1038/sj.npp.1301278.

Frank, M.J., Scheres, A., Sherman, S.J., 2007. Understanding decision-making deficits in neurological conditions: insights from models of natural action selection. Philosophical Transactions of the Royal Society B: Biological Sciences 362 (1485), 1641–1654. https://doi.org/10.1098/rstb.2007.2058.

Furukawa, E., da Costa, R.Q.M., Bado, P., Hoefle, S., Vigne, P., Monteiro, M., Wickens, J.R., Moll, J., Tripp, G., Mattos, P., 2020. Methylphenidate modifies reward cue responses in adults with ADHD: an fMRI study. Neuropharmacology 162, 107833. https://doi.org/10.1016/j.neuropharm.2019.107833.

Fusar-Poli, P., Rubia, K., Rossi, G., Sartori, G., Balottin, U., 2012. Striatal dopamine transporter alterations in ADHD: pathophysiology or adaptation to psychostimulants? a meta-analysis. Am. J. Psychiatry 169 (3), 264–272. https://doi.org/10.1176/appi.ajp.2011.11060940.

Ghahremani, D.G., Lee, B., Robertson, C.L., Tabibnia, G., Morgan, A.T., de Shetler, N., Brown, A.K., Monterosso, J.R., Aron, A.R., Mandelkern, M.A., Poldrack, R.A., London, E.D., 2012. Striatal dopamine D 2/D 3 receptors mediate response inhibition and related activity in frontostriatal neural circuitry in humans. Journal of Neuroscience 32 (21), 7316–7324. https://doi.org/10.1523/JNEUROSCI.4284-11.2012.

Greve, D.N., Fischl, B., 2009. Accurate and robust brain image alignment using boundary-based registration. NeuroImage 48 (1), 63–72. https://doi.org/10.1016/j.neuroimage.2009.06.060.

Gur, R.C., Richard, J., Hughett, P., Calkins, M.E., Macy, L., Bilker, W.B., Brensinger, C., Gur, R.E., 2010. A cognitive neuroscience-based computerized battery for efficient measurement of individual differences: standardization and initial construct validation. J. Neurosci. Methods 187 (2), 254–262. https://doi.org/10.1016/j.jneumeth.2009.11.017.

Gur, R.C., Richard, J., Calkins, M.E., Chiavacci, R., Hansen, J.A., Bilker, W.B., Loughead, J., Connolly, J.J., Qiu, H., Mentch, F.D., Abou-Sleiman, P.M., Hakonarson, H., Gur, R.E., 2012. Age group and sex differences in performance on a computerized neurocognitive battery in children age 8-21. Neuropsychology 26 (2), 251–265. https://doi.org/10.1037/a0026712.

Haacke, E.M., Cheng, N.Y.C., House, M.J., Liu, Q., Neelavalli, J., Ogg, R.J., Khan, A., Ayaz, M., Kirsch, W., Obenaus, A., 2005. Imaging iron stores in the brain using magnetic resonance imaging. Magn. Reson. Imaging 23 (1), 1–25. https://doi.org/10.1016/j.mri.2004.10.001.

Haacke, E.M., Miao, Y., Liu, M., Habib, C.A., Katkuri, Y., Liu, T., Yang, Z., Lang, Z., Hu, J., Wu, J., 2010. Correlation of putative iron content as represented by changes in R2* and phase with age in deep gray matter of healthy adults. J. Magn. Reson. Imaging: JMRI 32 (3), 561–576. https://doi.org/10.1002/jmri.22293.

Haber, S.N., 2003. The primate basal ganglia: parallel and integrative networks. J. Chem. Neuroanat. 26 (4), 317–330. https://doi.org/10.1016/j.jchemneu.2003.10.003.

Haber, S.N., Knutson, B., 2010. The Reward circuit: linking primate anatomy and human imaging. Neuropsychopharmacology 35 (1), 4–26. https://doi.org/10.1038/npp.2009.129.

Hallgren, B., Sourander, P., 1958. The effect of age on the non-haemin iron in the human brain. J. Neurochem. 3 (1), 41–51. https://doi.org/10.1111/j.1471-4159.1958.tb12607.x.

Hare, D., Ayton, S., Bush, A., Lei, P., 2013. A delicate balance: Iron metabolism and diseases of the brain. Front. Aging Neurosci. 5 (JUL), 1–19. https://doi.org/10.3389/fnagi.2013.00034.

Hasaneen, B.M., Sarhan, M., Samir, S., ELAssmy, M., Sakrana, A.A., Ashamalla, G.A., 2017. T2* magnetic resonance imaging: a non-invasive biomarker of brain iron content in children with attention-deficit/hyperactivity disorder. Egypt. J. Radiol. Nucl. Med. 48 (1), 161–167. https://doi.org/10.1016/j.ejrnm.2016.08.001.

Hect, J.L., Daugherty, A.M., Hermez, K.M., Thomason, M.E., 2018. Developmental variation in regional brain iron and its relation to cognitive functions in childhood. Dev. Cogn. Neurosci. 34, 18–26. https://doi.org/10.1016/j.dcn.2018.05.004.

Hofmans, L., Papadopetraki, D., van den Bosch, R., Määttä, J.I., Froböse, M.I., Zandbelt, B.B., Westbrook, A., Verkes, R.-J., Cools, R., 2020. Methylphenidate boosts choices of mental labor over leisure depending on striatal dopamine synthesis capacity. Neuropsychopharmacol.: Off. Publ. Am. Coll. Neuropsychopharmacol. 45 (13), 2170–2179. https://doi.org/10.1038/s41386-020-00834-1.

Huntenburg, J. (Freie U.B. (2014). Evaluating nonlinear coregistration of BOLD EPI and T1w images. ⟨http://hdl.handle.net/11858/00–001M-0000–002B-1CB5-A⟩.

Jenkinson, M., Beckmann, C.F., Behrens, T.E.J., Woolrich, M.W., Smith, S.M., 2012. FSL. NeuroImage 62 (2), 782–790. https://doi.org/10.1016/j.neuroimage.2011.09.015.

Kilbourn, M.R., 2014. In: Dierckx, R.A.J.O., Otte, A., de Vries, E.F.J., van Waarde, A., Luiten, P.G.M. (Eds.), Radioligands for Imaging Vesicular Monoamine Transporters BT - PET and SPECT of Neurobiological Systems. Springer, Berlin Heidelberg, pp. 765–790. https://doi.org/10.1007/978-3-642-42014-6_27.

Klein, A., Ghosh, S.S., Bao, F.S., Giard, J., Häme, Y., Stavsky, E., Lee, N., Rossa, B., Reuter, M., Chaibub Neto, E., Keshavan, A., 2017. Mindboggling morphometry of human brains. PLOS Comput. Biol. 13 (2), e1005350 https://doi.org/10.1371/journal.pcbi.1005350.

Larsen, B., Luna, B., 2015. In vivo evidence of neurophysiological maturation of the human adolescent striatum. In: Developmental Cognitive Neuroscience, Vol. 12. Elsevier Science,, pp. 74–85. https://doi.org/10.1016/j.dcn.2014.12.003.

Larsen, B., Olafsson, V., Calabro, F., Laymon, C., Tervo-Clemmens, B., Campbell, E., Minhas, D., Montez, D., Price, J., Luna, B., 2020. Maturation of the human striatal dopamine system revealed by PET and quantitative MRI. Nat. Commun. 11 (1), 846. https://doi.org/10.1038/s41467-020-14693-3.

Larsen, B., Bourque, J., Moore, T.M., Adebimpe, A., Calkins, M.E., Elliott, M.A., Gur, R. C., Gur, R.E., Moberg, P.J., Roalf, D.R., Ruparel, K., Turetsky, B.I., Vandekar, S.N., Wolf, D.H., Shinohara, R.T., Satterthwaite, T.D., 2020. Longitudinal development of brain iron is linked to cognition in youth. J. Neurosci. 40 (9), 1810 LP–1811818. https://doi.org/10.1523/JNEUROSCI.2434-19.2020.

Leth-Steensen, C., Elbaz, Z.K., Douglas, V.I., 2000. Mean response times, variability, and skew in the responding of ADHD children: a response time distributional approach. Acta Psychol. 104 (2), 167–190. https://doi.org/10.1016/s0001-6918(00)00019-6.

Lijffijt, M., Kenemans, J.L., Verbaten, M.N., van Engeland, H., 2005. A meta-analytic review of stopping performance in attention-deficit/hyperactivity disorder: deficient inhibitory motor control? J. Abnorm. Psychol. 114 (2), 216–222. https://doi.org/10.1037/0021-843X.114.2.216.

Luman, M., Oosterlaan, J., Sergeant, J.A., 2005. The impact of reinforcement contingencies on AD/HD: a review and theoretical appraisal. Clin. Psychol. Rev. 25 (2), 183–213. https://doi.org/10.1016/j.cpr.2004.11.001.

Ma, I., van Duijvenvoorde, A., Scheres, A., 2016. The interaction between reinforcement and inhibitory control in ADHD: A review and research guidelines. Clin. Psychol. Rev. 44, 94–111. https://doi.org/10.1016/j.cpr.2016.01.001.

Massidda, D. (2013). retimes: Reaction Time Analysis.

Mink, J.W., 1996. The Basal Ganglia: Focused selection and inhibition of competing motor programs. Progress in Neurobiology 50 (4), 381–425. https://doi.org/10.1016/S0301-0082(96)00042-1.

Mostofsky, S.H., Simmonds, D.J., 2008. Response inhibition and response selection: two sides of the same coin. J. Cogn. Neurosci. 20 (5), 751–761. https://doi.org/10.1162/jocn.2008.20500.

Nagatsu, T., Levitt, M., Udenfriend, S., 1964. Tyrosine hydroxylase. The initial step in norephinephrine biosynthesis. J. Biol. Chem. 239, 2910–2917.

Nieoullon, A., 2002. Dopamine and the regulation of cognition and attention. Prog. Neurobiol. 67 (1), 53–83. https://doi.org/10.1016/s0301-0082(02)00011-4.

Oosterlaan, J., Logan, G.D., Sergeant, J.A., 1998. Response inhibition in AD/HD, CD, comorbid AD/HD + CD, anxious, and control children: a meta-analysis of studies with the stop task. J. Child Psychol. Psychiatry Allied Discip. 39 (3), 411–425. https://doi.org/10.1017/S0021963097002072.

Ortega, R., Cloetens, P., Devès, G., Carmona, A., Bohic, S., 2007. Iron storage within dopamine neurovesicles revealed by chemical nano-imaging. PLOS ONE 2 (9), e925. https://doi.org/10.1371/journal.pone.0000925.

Padmanabhan, A., Luna, B., 2014. Developmental imaging genetics: linking dopamine function to adolescent behavior. Brain and cognition 89, 27–38. https://doi.org/10.1016/j.bandc.2013.09.011.

Parr, A.C., Calabro, F., Tervo-Clemmens, B., Larsen, B., Foran, W., Luna, B., 2022. Contributions of dopamine-related basal ganglia neurophysiology to the developmental effects of incentives on inhibitory control. Dev. Cogn. Neurosci. 54, 101100 https://doi.org/10.1016/j.dcn.2022.101100.

Peirce, J.W., 2007. PsychoPy—Psychophysics software in Python. J. Neurosci. Methods 162 (1), 8–13. https://doi.org/10.1016/j.jneumeth.2006.11.017.

Peirce, J.W., 2009. Generating stimuli for neuroscience using PsychoPy. Front. Neuroinformatics 2. https://doi.org/10.3389/neuro.11.010.2008.

Peterson, E.T., Kwon, D., Luna, B., Larsen, B., Prouty, D., De Bellis, M.D., Voydovic, J., Liu, C., Li, W., Pohl, K.M., Sullivan, E.V., Pfefferbaum, A., 2019. Distribution of brain iron accrual in adolescence: Evidence from cross-sectional and longitudinal analysis. Hum. Brain Mapp. 40 (5), 1480–1495. https://doi.org/10.1002/hbm.24461.

Philipp-Wiegmann, F., Rösler, M., Clasen, O., Zinnow, T., Retz-Junginger, P., Retz, W., 2018. ADHD modulates the course of delinquency: a 15-year follow-up study of young incarcerated man. Eur. Arch. Psychiatry Clin. Neurosci. 268 (4), 391–399. https://doi.org/10.1007/s00406-017-0816-8.

Polanczyk, G., Silva de Lima, M., Horta, B.L., Biederman, J., Rohde, L.A., 2007. Worldwide prevalence of ADHD: A systematic review and metaregression analysis. Am. J. Psychiatry 164, 942–948.

Power, J.D., Mitra, A., Laumann, T.O., Snyder, A.Z., Schlaggar, B.L., Petersen, S.E., 2014. Methods to detect, characterize, and remove motion artifact in resting state fMRI. NeuroImage 84, 320–341. https://doi.org/10.1016/j.neuroimage.2013.08.048.

Price, R.B., Tervo-Clemmens, B.C., Panny, B., Degutis, M., Griffo, A., Woody, M., 2021. Biobehavioral correlates of an fMRI index of striatal tissue iron in depressed patients. Transl. Psychiatry 11 (1), 448. https://doi.org/10.1038/s41398-021-01553-x.

Rapport, M.D., Alderson, R.M., Kofler, M.J., Sarver, D.E., Bolden, J., Sims, V., 2008. Working memory deficits in boys with attention-deficit/hyperactivity disorder (ADHD): the contribution of central executive and subsystem processes. J. Abnorm. Child Psychol. 36 (6), 825–837. https://doi.org/10.1007/s10802-008-9215-y.

Reuter, M., Rosas, H.D., Fischl, B., 2010. Highly accurate inverse consistent registration: a robust approach. NeuroImage 53 (4), 1181–1196. https://doi.org/10.1016/j.neuroimage.2010.07.020.

Rosch, K.S., Fosco, W.D., Pelham, W.E., Waxmonsky, J.G., Bubnik, M.G., Hawk, L.W., 2016. Reinforcement and stimulant medication ameliorate deficient response inhibition in children with attention-deficit/hyperactivity disorder. J. Abnorm. Child Psychol. 44 (2), 309–321. https://doi.org/10.1007/s10802-015-0031-x.

Rubia, K., Halari, R., Cubillo, A., Mohammad, A.-M., Brammer, M., Taylor, E., 2009. Methylphenidate normalises activation and functional connectivity deficits in attention and motivation networks in medication-naïve children with ADHD during a rewarded continuous performance task. Neuropharmacology 57 (7–8), 640–652. https://doi.org/10.1016/j.neuropharm.2009.08.013.

Schipper, H.M., 2012. Neurodegeneration with brain iron accumulation — clinical syndromes and neuroimaging. Biochim. Et. Biophys. Acta (BBA) - Mol. Basis Dis. 1822 (3), 350–360. https://doi.org/10.1016/j.bbadis.2011.06.016.

Shaffer, D., Fisher, P., Lucas, C.P., Dulcan, M.K., Schwab-Stone, M.E., 2000. NIMH Diagnostic Interview Schedule for Children Version IV (NIMH DISC- IV): Description, differences from previous versions, and reliability of some common diagnoses. J. Am. Acad. Child Adolesc. Psychiatry 39 (1), 28–38. https://doi.org/10.1097/00004583-200001000-00014.

Shapiro, S.S., Wilk, M.B., 1965. An analysis of variance test for normality (complete samples. Biometrika 52 (3/4), 591–611. https://doi.org/10.2307/2333709.

Shiels-Rosch, K., Hawk Jr., L.W., 2013. The effects of performance-based rewards on neurophysiological correlates of stimulus, error, and feedback processing in children with ADHD. Psychophysiology 50 (11), 1157–1173. https://doi.org/10.1111/psyp.12127.

Siegel, J.S., Power, J.D., Dubis, J.W., Vogel, A.C., Church, J.A., Schlaggar, B.L., Petersen, S.E., 2014. Statistical improvements in functional magnetic resonance imaging analyses produced by censoring high-motion data points. Hum. Brain Mapp. 35 (5), 1981–1996. https://doi.org/10.1002/hbm.22307.

Spanagel, R., Weiss, F., 1999. The dopamine hypothesis of reward: Past and current status. In: Trends in Neurosciences, Vol. 22. Elsevier Science,, pp. 521–527. https://doi.org/10.1016/S0166-2236(99)01447-2.

Tamm, L., Carlson, C.L., 2007. Task demands interact with the single and combined effects of medication and contingencies on children With ADHD. J. Atten. Disord. 10 (4), 372–380. https://doi.org/10.1177/1087054706289946.

Tekin, S., Cummings, J.L., 2002. Frontal-Subcortical Neuronal Circuits and Clinical Neuropsychiatry: An update. In: Journal of Psychosomatic Research, Vol. 53. Elsevier Science, pp. 647–654. https://doi.org/10.1016/S0022-3999(02)00428-2.

Treiber, J.M., White, N.S., Steed, T.C., Bartsch, H., Holland, D., Farid, N., McDonald, C. R., Carter, B.S., Dale, A.M., Chen, C.C., 2016. Characterization and correction of geometric distortions in 814 diffusion weighted images. PLOS ONE 11 (3), e0152472. https://doi.org/10.1371/journal.pone.0152472.

Tustison, N.J., Avants, B.B., Cook, P.A., Zheng, Y., Egan, A., Yushkevich, P.A., Gee, J.C., 2010. N4ITK: Improved N3 bias correction. IEEE Trans. Med. Imaging 29 (6), 1310–1320. https://doi.org/10.1109/TMI.2010.2046908.

Vo, L.T.K., Walther, D.B., Kramer, A.F., Erickson, K.I., Boot, W.R., Voss, M.W., Prakash, R.S., Lee, H., Fabiani, M., Gratton, G., Simons, D.J., Sutton, B.P., Wang, M. Y., 2011. Predicting individuals' learning success from patterns of pre-learning MRI activity. PLOS ONE 6 (1), e16093. https://doi.org/10.1371/journal.pone.0016093.

Volkow, N., Wang, G.-J., Fowler, J.S., Thanos, P.P.K., Logan, J., Gatley, S.J., Gifford, A., Ding, Y.-S., Wong, C., Pappas, N., 2002. Brain DA D2 receptors predict reinforcing effects of stimulants in humans: replication study. Synap. (N., Y., N. Y.) 46 (2), 79–82. https://doi.org/10.1002/syn.10137.

Volkow, N., Fowler, J.S., Wang, G.-J., Ding, Y.-S., Gatley, S.J., 2002a. Role of dopamine in the therapeutic and reinforcing effects of methylphenidate in humans: results from imaging studies. Eur. Neuropsychopharmacol. 12 (6), 557–566. https://doi.org/10.1016/S0924-977X(02)00104-9.

Volkow, N., Fowler, J.S., Wang, G.-J., Ding, Y., Gatley, S.J., 2002b. Mechanism of action of methylphenidate: Insights from PET imaging studies. J. Atten. Disord. 6 (1_suppl), 31–43. https://doi.org/10.1177/070674370200601S05.

Volkow, N., Wang, G.-J., Newcorn, J., Telang, F., Solanto, M.V., Fowler, J.S., Logan, J., Ma, Y., Schulz, K., Pradhan, K., Wong, C., Swanson, J.M., 2007. Depressed Dopamine Activity in Caudate and Preliminary Evidence of Limbic Involvement in Adults With Attention-Deficit/Hyperactivity Disorder. Arch. Gen. Psychiatry 64 (8), 932–940. https://doi.org/10.1001/archpsyc.64.8.932.

Volkow, N., Fowler, J.S., Wang, G.-J., Kollins, S.H., Wigal, T.L., Newcorn, J.H., Telang, F., Fowler, J. S., Zhu, W., Logan, J., Ma, Y., Pradhan, K., Wong, C., Swanson, J.M., 2009. Evaluating dopamine reward pathway in ADHD: Clinical implications. JAMA 302 (10), 1084–1091. https://doi.org/10.1001/jama.2009.1308.

Volkow, N., Wang, G.-J., Newcorn, J.H., Kollins, S.H., Wigal, T.L., Telang, F., Fowler, J. S., Goldstein, R.Z., Klein, N., Logan, J., Wong, C., Swanson, J.M., 2011. Motivation deficit in ADHD is associated with dysfunction of the dopamine reward pathway. Mol. Psychiatry 16 (11), 1147–1154. https://doi.org/10.1038/mp.2010.97.

Wahlstrom, D., Collins, P., White, T., Luciana, M., 2010. Developmental changes in dopamine neurotransmission in adolescence: Behavioral implications and issues in assessment. Brain and Cognition 72 (1), 146–159. https://doi.org/10.1016/j.bandc.2009.10.013.

Wang, S., Peterson, D.J., Gatenby, J.C., Li, W., Grabowski, T.J., Madhyastha, T.M., 2017. Evaluation of field map and nonlinear registration methods for correction of susceptibility artifacts in diffusion MRI. Front. Neuroinformatics Vol. 11. https://doi.org/10.3389/fninf.2017.00017.

Wechsler, D., 1992. Wechsler individual achievement test. Psychological Corporation,, San Antonio, TX.

Wechsler, D., 2014. WISC-V: Technical and interpretive manual. NCS Pearson, Inc.

Winter, W., Sheridan, M., 2014. Previous reward decreases errors of commission on later 'No-Go' trials in children 4 to 12 years of age: evidence for a context monitoring account. Developmental Science 17 (5), 797–807. https://doi.org/10.1111/desc.12168.

Zandbelt, B.B., Vink, M., 2010. On the role of the striatum in response inhibition. PloS One 5 (11). https://doi.org/10.1371/journal.pone.0013848.

Zhang, Y., Brady, M., Smith, S., 2001. Segmentation of brain MR images through a hidden Markov random field model and the expectation-maximization algorithm. IEEE Trans. Med. Imaging 20 (1), 45–57. https://doi.org/10.1109/42.906424.